


---


# A SIMPLE ALGEBRAIC SOLUTION FOR ESTIMATING THE POSE OF A CAMERA FROM PLANAR POINT FEATURES

---

AUTHOR ACCEPTED VERSION\*

 **Tarek Bouazza**  
I3S, CNRS, Université Côte d'Azur  
Sophia Antipolis, France  
bouazza@i3s.unice.fr

 **Tarek Hamel**  
I3S, CNRS, Université Côte d'Azur  
and Insitut Universitaire de France  
Sophia Antipolis, France  
thamel@i3s.unice.fr

 **Claude Samson**  
INRIA Sophia Antipolis and I3S  
Sophia Antipolis, France  
csamson@i3s.unice.fr

August 5, 2025

## ABSTRACT

This paper presents a simple algebraic method to estimate the pose of a camera relative to a planar target from  $n \geq 4$  reference points with known coordinates in the target frame and their corresponding bearing measurements in the camera frame. The proposed approach follows a hierarchical structure; first, the unit vector normal to the target plane is determined, followed by the camera's position vector, its distance to the target plane, and finally, the full orientation. To improve the method's robustness to measurement noise, an averaging methodology is introduced to refine the estimation of the target's normal direction. The accuracy and robustness of the approach are validated through extensive experiments.

## 1 Introduction

Vision-based motion estimation is a central issue in robotics that involves reconstructing the pose, i.e., position and orientation, of a mobile camera. Given correspondences between the 3D coordinates of  $n$  reference points in an object frame and their image projections, this problem is known as the Perspective- $n$ -Point (PnP) problem, as introduced by Fischler and Bolles [1981]. Solutions to the PnP problem are typically categorized according to the number of reference points. The simplest case, the P3P problem ( $n = 3$ ) has been extensively studied [Fischler and Bolles [1981], Gao et al. [2003], Kneip et al. [2011]]. At best (when the points are non-collinear), there are four possible solutions [Zhang and Hu [2005]]. A fourth non-coplanar point is required to resolve the ambiguity and uniquely determine the pose.

For  $n \geq 4$ , the problem usually admits a unique solution, except in some degenerate configurations (e.g., collinear or coplanar points). Methods which solve the general PnP problem exploit the redundancy of more correspondences to achieve higher accuracy. Early non-iterative approaches provide explicit closed-form solutions to compute the camera pose directly [Quan and Lan [1999]]. Iterative algorithms have also been developed to determine the camera pose by minimizing an appropriate cost function (e.g., the reprojection error of the points), such as Haralick et al. [1989], the POSIT iterative algorithm [DeMenthon and Davis [1995]], the RPP introduced by Lu et al. [2000], and the SDP method [Schweighofer and Pinz [2008]]. The drawback of these latter methods is their high computational cost and the need for a good initialization to avoid local minima. The EPnP method proposed by Lepetit et al. [2009] was among the earliest efficient non-iterative solutions that achieve a computational cost of  $O(n)$  by expressing the  $n$  reference points as a weighted sum of four virtual control points. Subsequent methods with linear complexity, such as DLS [Hesch and Roumeliotis [2011]], RPnP [Li et al. [2012]], and UPnP [Kneip et al. [2014]], were developed to improve the precision by replacing the linear formulation with polynomial solvers. The nonstationary case of the PnP problem was investigated by the co-authors in Hamel and Samson [2017], where the point correspondences were combined with the camera's rigid motion and its velocity measurements to design continuous-time filters.

---

\*Bouazza, T., et al. (2025), "A Simple Algebraic Solution for Estimating the Pose of a Camera from Planar Point Features", *Accepted for presentation at IEEE/RSJ International Conference on Intelligent Robots and Systems (IROS)*.

©2025 IEEE. Personal use of this material is permitted. Permission from IEEE must be obtained for all other uses, in any current or future media, including reprinting/republishing this material for advertising or promotional purposes, creating new collective works, for resale or redistribution to servers or lists, or reuse of any copyrighted component of this work in other works.

The PnP problem is typically classified into planar and nonplanar cases. Apart from recent non-iterative methods like EPnP that include special cases when the  $n$  points are coplanar, most PnP algorithms are not suitable for planar configurations and tend to perform suboptimally. Solutions that were specifically designed for the planar PnP problem include the extension of the POSIT algorithm DeMenthon and Davis [1995] to coplanar points Oberkampf et al. [1996] and the solution proposed in Schweighofer and Pinz [2006] which extends the RPP method Lu et al. [2000]. Alternatively, solvers that assume coplanarity, such as the IPPE Collins and Bartoli [2014], are based on the plane-to-image homography transformation Hartley and Zisserman [2003] and take advantage of the planar structure to achieve higher accuracy. Another common strategy to plane-based pose estimation is homography decomposition, where the homography matrix is first computed, e.g. using the Direct Linear Transform (DLT) method Hartley and Zisserman [2003], and then factorized to recover the camera pose using either SVD-based Faugeras and Lustman [1988], Zhang and Hanson [1996] or analytical methods Malis and Vargas [2007].

This paper presents a simple algebraic method to compute the pose of a camera relative to a planar target, as well as determining the distance and normal vector of the target plane, using the coordinates of  $n \geq 4$  reference points in the target frame and their corresponding bearing measurements in the camera frame. The method follows a hierarchical structure in retrieving the relative pose parameters, the unit vector normal to the target plane is first estimated from one of several sets of four points, then the camera's position vector and distance to the plane are recovered, and finally its orientation. A key advantage of the proposed formulation is its ability to recover partial pose information (e.g., direction of the position vector) even when the camera is considerably far from the target and the normal, and subsequently the orientation, are poorly estimated. This direction information could be exploited in control applications, such as the approach to and landing on a planar target, by providing an initial estimate to align the camera with the target frame. Additionally, when combined with an onboard IMU, this method can be extended to design a filter for the estimation of the inertial velocity relative to a slowly accelerating target.

The remainder of the paper is organized as follows. Section 2 introduces the preliminary notation and Section 3 formally states the problem and outlines the key stages of the proposed algorithm. Section 4 presents the experimental validation, followed by concluding remarks in Section 5.

## 2 Preliminary notation

Throughout the paper,  $E^3$  denotes the 3D Euclidean vector space and vectors in  $E^3$  are denoted with bold letters. The associated reference frame is an inertial frame with respect to (w.r.t.) which all other frames are defined. The inner product in  $E^3$  is denoted by “ $\cdot$ ”. The following notation is used.

- For  $x \in \mathbb{R}^n$  (resp.  $\mathbf{x} \in E^3$ )  $|x|$  (resp.  $|\mathbf{x}|$ ) denotes the Euclidean norm, and  $x^\top$  denotes the transpose of  $x$ .
- $C$  denotes the camera's optical center;
- $\mathcal{F}_c = \{C; \mathbf{v}_c, \mathbf{j}_c, \mathbf{k}_c\}$  is the camera frame with  $\mathbf{k}_c$  orthogonal to the camera's image plane;
- $\mathcal{F}_t = \{O; \mathbf{v}_t, \mathbf{j}_t, \mathbf{k}_t\}$  is a frame attached to the target, with the origin  $O$  on the target plane and  $\mathbf{k}_t$  orthogonal to the target plane;
- $\mathbf{SO}(3) := \{R \in \mathbb{R}^{3 \times 3} \mid R^\top R = I_3, \det(R) = 1\}$  is the special orthogonal group of 3D rotation.
- $R \in \mathbf{SO}(3)$  is the rotation matrix from  $\mathcal{F}_t$  to  $\mathcal{F}_c$ , i.e.  $(\mathbf{v}_c, \mathbf{j}_c, \mathbf{k}_c) = (\mathbf{v}_t, \mathbf{j}_t, \mathbf{k}_t)R$ .
- $\xi \in \mathbb{R}^3$  is the 3d-vector of coordinates of the camera position expressed in the basis of the camera frame, i.e.  $\vec{OC} = (\mathbf{v}_c, \mathbf{j}_c, \mathbf{k}_c)\xi$ .
- $x_i \in \mathbb{R}^2$  is the 2d-vector of coordinates of the point  $P_i$  on the target plane, expressed in the basis of the target frame. The corresponding coordinates in  $\mathbb{R}^3$  are given by  $\hat{x}_i = (x_i^\top, 0)^\top$ , i.e.  $\vec{OP}_i = (\mathbf{v}_t, \mathbf{j}_t, \mathbf{k}_t)\hat{x}_i$ . The homogeneous coordinates of  $x_i$  are  $\bar{x}_i = (x_i^\top, 1)^\top$ .
- $S^2 := \{p \in \mathbb{R}^3 \mid |p| = 1\}$  denotes the unit sphere that consists of all unit vectors in  $\mathbb{R}^3$ .
- $e_3 = (0, 0, 1)^\top \in S^2$ .
- $p_i \in S^2$  is the 3d-unit vector of coordinates of the bearing of the point  $P_i$  expressed in the basis of the camera frame, i.e.  $C\vec{P}_i / |C\vec{P}_i| = (\mathbf{v}_c, \mathbf{j}_c, \mathbf{k}_c)p_i$ , computed from the calibrated image coordinates  $y_i = (u_x, u_y)$  of  $P_i$  as  $p_i = (u_x, u_y, 1)^\top / \sqrt{u_x^2 + u_y^2 + 1}$ .
- $\eta \in S^2$  is the vector of coordinates of the unit vector  $\mathbf{k}_t$  expressed in the basis of the camera frame. Since  $\mathbf{k}_t = (\mathbf{v}_t, \mathbf{j}_t, \mathbf{k}_t)e_3 = (\mathbf{v}_c, \mathbf{j}_c, \mathbf{k}_c)R^\top e_3$ , then  $\eta = R^\top e_3$ .
- $d$  is the distance between the camera's optical center and the target plane. Since  $d = \vec{CO} \cdot \mathbf{k}_t$  with  $\vec{CO} = -(\mathbf{v}_c, \mathbf{j}_c, \mathbf{k}_c)\xi$  and  $\mathbf{k}_t = (\mathbf{v}_c, \mathbf{j}_c, \mathbf{k}_c)\eta$ , then  $d = -\eta^\top \xi$ .



Define  $\hat{x}_{ij} := \hat{x}_j - \hat{x}_i$ , for  $i, j \in \{1, \dots, 4\}$ . From (1)

$$d \left( \frac{p_1}{\eta^\top p_1} - \frac{p_i}{\eta^\top p_i} \right) = R^\top \hat{x}_{1i}, \quad i = 2, 3, 4. \quad (2)$$

Determine  $\lambda_i \in \mathbb{R}$ ,  $i = 2, 3, 4$ , such that  $\sum_{i=2}^4 \lambda_i \hat{x}_{1i} = 0$  and  $\sum_{i=2}^4 \lambda_i = 1$ . These coefficients regrouped in the vector  $\lambda = (\lambda_2, \lambda_3, \lambda_4)^\top$  are, for instance, given by  $\lambda = X^{-1}e_3$ , where  $X \in \mathbb{R}^{3 \times 3}$  is the invertible matrix defined by

$$X := \begin{bmatrix} \bar{x}_{12} & \bar{x}_{13} & \bar{x}_{14} \end{bmatrix}.$$

Using the definition of  $\lambda_i$ ,  $i = 2, 3, 4$ , one deduces from (2)

$$d \left( \frac{p_1}{\eta^\top p_1} - \sum_{i=2}^4 \lambda_i \frac{p_i}{\eta^\top p_i} \right) = 0$$

and, since  $d \neq 0$

$$p_1 = (\eta^\top p_1) \sum_{i=2}^4 \lambda_i \frac{p_i}{\eta^\top p_i}, \quad (3)$$

with  $\eta^\top p_1 > 0$ . On the other hand, since the points  $P_2$ ,  $P_3$ , and  $P_4$  are not aligned, the corresponding bearing vectors  $p_2$ ,  $p_3$ , and  $p_4$  are independent in  $\mathbb{R}^3$  and thus constitute a spanning set of  $\mathbb{R}^3$ . Therefore, there exists a *unique* vector of non-zero coefficients  $a = (a_2, a_3, a_4) \in \mathbb{R}^3$  such that

$$p_1 = \sum_{i=2}^4 a_i p_i. \quad (4)$$

Defining the invertible matrix  $B := [p_2 \ p_3 \ p_4]$ , the vector  $a$  is given by  $a = B^{-1}p_1$ . By identifying the coefficients in the right-hand side of (3) and (4) one gets

$$a_i = (\eta^\top p_1) \lambda_i \frac{p_i}{\eta^\top p_i}, \quad i = 2, 3, 4.$$

This also implies that  $p_i^\top \eta = (\eta^\top p_1) \lambda_i / a_i$ ,  $i = 2, 3, 4$ , or, equivalently

$$B^\top \eta = (\eta^\top p_1) b, \quad (5)$$

with  $b = (\lambda_2/a_2, \lambda_3/a_3, \lambda_4/a_4)^\top$ . Therefore, given that  $\eta$  is a unit vector and that  $\eta^\top p_1 > 0$ , one obtains

$$\eta = B^{-\top} b / |B^{-\top} b|. \quad (6)$$

Note that any other set of four points (with no three collinear points) can be used to compute  $\eta$ . If the bearings  $p_i$  were exact projections of the matched image points  $y_i$ , all estimates of  $\eta$  would coincide. However, in practice, these measurements are imperfect because of pixel noise. For this reason, it may be useful to collect as many estimates  $\hat{\eta}_j$  as there are different sets of four matched points and calculate a final estimate of  $\eta$  as a weighted sum of  $\hat{\eta}_j$ , i.e.

$$\hat{\eta} = \sum_{j=1}^m \gamma_j \hat{\eta}_j / \left| \sum_{j=1}^m \gamma_j \hat{\eta}_j \right|, \quad (7)$$

where  $\gamma_j > 0$  represents the weight (confidence) assigned to the  $j$ th estimate  $\hat{\eta}_j$ . A natural choice for  $\gamma_j$  is given by  $\gamma_j = |\min_{i=2,3,4} (a_{i,j}) \det(B_j)|$ , which gives higher confidence to estimates derived from sets of points that are more widely distributed in the planar target.

Another option is pointed out next. Let  $m$  denote the number of four points sets used to estimate  $\eta$ , and  $j = 1, \dots, m$  the ordering index attributed to these sets. Accordingly, specifying (5) for each set yields

$$B_j^\top \eta = (\eta^\top p_{1,j}) b_j, \quad j = 1, \dots, m.$$

This latter relation in turn implies

$$D\eta = 0, \quad (8)$$

with  $D \in \mathbb{R}^{3m \times 3}$  defined by

$$D := \begin{bmatrix} \gamma_1 (B_1 - p_{1,1}^\top b_1) \\ \vdots \\ \gamma_m (B_m - p_{1,m}^\top b_m) \end{bmatrix}.$$

Equation (8) indicates that  $\eta$  is the unit eigenvector associated with the null eigenvalue of the semi-positive matrix  $D^\top D \in \mathbb{R}^{3 \times 3}$ . This suggests setting  $\hat{\eta}$  as the normalized eigenvector associated with the smallest eigenvalue of  $D^\top D$ , which may be non-zero due to pixel noise.

**Remark 1.** Directly computing  $\hat{\eta}$  as a weighted sum in  $\mathbb{R}^3$  can lead to errors, especially when individual estimates are affected by measurement noise. An averaging methodology that guarantees robustness to noise and smoother convergence (called smooth averaging) accounts for the fact that  $\eta$  lies on the unit sphere  $S^2$ . Given estimates  $\hat{\eta}_j$ ,  $j = 1, \dots, m$ , from a new image, the prior  $\hat{\eta}$  is refined by

$$\hat{\eta} \leftarrow \exp(\sigma^\times) \hat{\eta}, \quad \sigma = - \sum_{j=1}^m \gamma_j (\hat{\eta} \times \hat{\eta}_j), \quad (9)$$

where  $\exp((\cdot)^\times) : \mathbb{R}^3 \rightarrow \mathbf{SO}(3)$  is the matrix exponential map computed using Rodrigues' formula Hartley and Zisserman [2003], and  $\hat{\eta}(0)$  can be taken from the first image according to (7). This update corresponds to the solution of the minimization problem

$$\operatorname{argmin}_{\eta \in S^2} \frac{1}{2} \sum_{j=1}^m \gamma_j |\hat{\eta}_j - \eta|^2.$$

Alternatively, the update (9) can be applied sequentially for each measurement  $\hat{\eta}_j$  obtained from a set of four points to refine  $\hat{\eta}$  as  $\hat{\eta} \leftarrow \exp(\gamma_j (\hat{\eta} \times \hat{\eta}_j)^\times) \hat{\eta}$ ,  $j = 1, \dots, m$ . However, this comes at the cost of increased computation, since the exponential map must be evaluated  $m$  times rather than once.

### 3.0.2 Calculation of $d$ and $\xi$

Assume now that  $\eta$ , or an accurate estimate of it, is known. Consider  $n \geq 4$  matched points  $P_i$ ,  $i = 1, \dots, n$ , such that at least three are non-collinear. Determine a set of coefficients  $\mu_i$ ,  $i = 1, \dots, n$ , such that  $\sum_{i=1}^n \mu_i x_i = 0$  and  $\sum_{i=1}^n \mu_i = 1$ . Regrouped into the  $n$ -dimensional vector  $\mu = (\mu_1, \dots, \mu_n)^\top$ , a (non unique) set of such coefficients is given by  $\mu = \bar{X}^\dagger e_3$ , where  $\bar{X} \in \mathbb{R}^{3 \times n}$  is defined by

$$\bar{X} := [\bar{x}_1 \quad \dots \quad \bar{x}_n],$$

and  $\bar{X}^\dagger = \bar{X}^\top (\bar{X} \bar{X}^\top)^{-1}$  is a pseudo-inverse of  $\bar{X}$ . Note that  $\bar{X} \bar{X}^\top \in \mathbb{R}^{3 \times 3}$  is invertible due to the assumption on the chosen set of matched points. Now, define and compute the following vector

$$r := \sum_{i=1}^n \frac{\mu_i}{\eta^\top p_i} p_i. \quad (10)$$

One deduces from (1) that

$$\xi = -dr. \quad (11)$$

From (1), one has also

$$R^\top \hat{x}_i = \xi + \frac{d}{\eta^\top p_i} p_i, \quad \forall i = 1, \dots, n.$$

Therefore,  $R^\top \hat{x}_i = dq_i$  with

$$q_i := \frac{1}{\eta^\top p_i} p_i - r. \quad (12)$$

and

$$d = \frac{|\hat{x}_i|}{|q_i|}, \quad \forall i = 1, \dots, n. \quad (13)$$

From the previous three relations

$$R^\top \frac{\hat{x}_i}{|\hat{x}_i|} = \frac{q_i}{|q_i|}. \quad (14)$$

Note that relation (13) also implies that

$$d = \frac{1}{n} \sum_{i=1}^n \frac{|\hat{x}_i|}{|q_i|}. \quad (15)$$

Due to imperfect measurements in the image, this averaged solution, or a weighted variant, will be preferred in practice. Once  $d$  is determined,  $\xi$  can be directly obtained using (11).

**Remark 2.** When the distance between the camera and the origin of the target plane becomes large, all matched points bearings  $p_i$  tend to  $-\xi/|\xi|$ . This is coherent with relations (10) and (13) according to which  $r = -\xi/|\xi|$ . This is true even when  $\eta$ , and subsequently the orientation of the camera w.r.t. the target frame, are no longer well estimated due to image noise and poor conditioning of the matrix  $B$ . The fact that  $r$  continues to be a good estimate of the direction  $-\xi/|\xi|$  is a practical asset of the proposed algorithm that can, for instance, be exploited to control the approach of a camera-equipped-vehicle towards the origin of the target plane when the inertial orientation of the vehicle is independently estimated by using IMU measurements.

### 3.0.3 Calculation of $R$

For this third stage, assume that  $\eta$  and  $\xi$  are known. As before, consider a set of  $n \geq 4$  matched points  $P_i, i = 1, \dots, n$ , such that at least three of them are non-collinear. Note that there is no requirement of choosing the same set of points as those used in previous stages. As a matter of fact, any two matched points not collinear with the origin of the target frame are sufficient. Define the matrix

$$\bar{X} := \begin{bmatrix} \hat{x}_1 & \dots & \hat{x}_n \\ |\hat{x}_1| & \dots & |\hat{x}_n| \end{bmatrix} e_3 \in \mathbb{R}^{3 \times n+1}, \quad (16)$$

which is of rank three because of the assumption on the chosen set of matched points. From (14) and the definition of  $\eta$ , i.e.  $\eta = R^\top e_3$ ,  $R^\top \bar{X} = Y$ , with

$$Y := \begin{bmatrix} q_1 & \dots & q_n \\ |q_1| & \dots & |q_n| \end{bmatrix} \eta. \quad (17)$$

Therefore

$$R^\top = Y \bar{X}^\dagger, \quad (18)$$

with  $\bar{X}^\dagger := \bar{X}^\top (\bar{X} \bar{X}^\top)^{-1}$ .

Measurement noise can cause the computed matrix  $R^\top$  to deviate from a true rotation matrix in  $\mathbf{SO}(3)$ . To correct this, a regularization step is needed. For instance, a Gram-Schmidt orthonormalization procedure can be applied, using the fact that the last column of  $R^\top$ , i.e.  $R^\top e_3$ , is equal to  $\eta$ .

**Remark 3.** Similar to Remark 1, the orientation  $R$  can be estimated through a smooth averaging procedure rather than an algebraic computation, exploiting the relation  $\eta = R^\top e_3$ . In this case, the full orientation can be determined from the additional knowledge of the  $n$  vectors  $q_i/|q_i|$  and relation (14). This step is omitted here, as the resulting yaw estimates are already sufficiently accurate for the intended purpose.

**Remark 4.** The homography matrix, which relates the bearings of matched points between two images of a planar structure Hartley and Zisserman [2003], can also be derived from (1). For the bearings  $p_{i,1}$  and  $p_{i,2}$  of a point  $P_i$  observed in two images, one has

$$\frac{d_j}{\eta_j^\top p_{i,j}} p_{i,j} = R_j^\top (\hat{x}_i - \xi_j^t), \quad j = 1, 2$$

with  $\xi_j^t$  denoting the coordinates of  $CP_i$  expressed in the target frame. From this latter relation

$$R \frac{d_1}{\eta_1^\top p_{i,1}} p_{i,1} - \frac{d_2}{\eta_2^\top p_{i,2}} p_{i,2} = -\tilde{\xi}$$

with  $\tilde{R} = R_2^\top R_1$ , the relative rotation between the two camera frames, and  $\tilde{\xi} = R_2^\top (\xi_1^t - \xi_2^t)$ , the relative translation vector expressed in the frame of image 2. Multiplying both members of this latter equality by  $\frac{\eta_1^\top p_{i,1}}{d_1}$  yields

$$\gamma_i p_{i,2} = H p_{i,1} \quad (19)$$

where  $H := \tilde{R} + \frac{\tilde{\xi} \eta_1^\top}{d_1} \in \mathbb{R}^{3 \times 3}$  is the homography matrix, and  $\gamma_i = \frac{\eta_1^\top p_{i,1}}{\eta_2^\top p_{i,2}} \frac{d_2}{d_1}$ . Relation (19) indicates that  $H$ , which may be assimilated to an element of the special linear group  $\mathbf{SL}(3)$  (an 8-dimensional matrix Lie group) after re-scaling to  $\bar{H} := H \det(H)^{-\frac{1}{3}}$ , can be determined from the knowledge of four, or more, bearing pairs  $(p_{i,1}, p_{i,2})$  Hartley and Zisserman [2003]. Once estimated,  $H$  can in turn be decomposed Malis and Vargas [2007] to extract the rotation  $\tilde{R}$ , the unit normal  $\eta_1$ , and the scaled displacement  $\frac{\tilde{\xi}}{d_1}$ .

## 4 Experimental validation

In this section, we present experimental results to demonstrate the performance of the proposed algorithm on real image data. The experiments were performed using a calibrated Basler ace camera that captures images at 20 frames per second with a resolution of  $640 \times 512$  pixels. The point detection was performed with the ArUco library Romero-Ramirez et al. [2018] included in OpenCV, which provides reliable corner detection from fiducial markers. The target consisted of a set of 38 fiducial markers (dictionary: DICT\_4X4\_50) of varying sizes arranged on a  $23.5 \times 18.8$  cm planar board (Fig. 2).

The algorithm was implemented in C++ using the Eigen matrix library. The ground-truth pose measurements were obtained using an OptiTrack motion capture (MoCap) system at a rate of 100Hz, with markers attached to both the camera and the

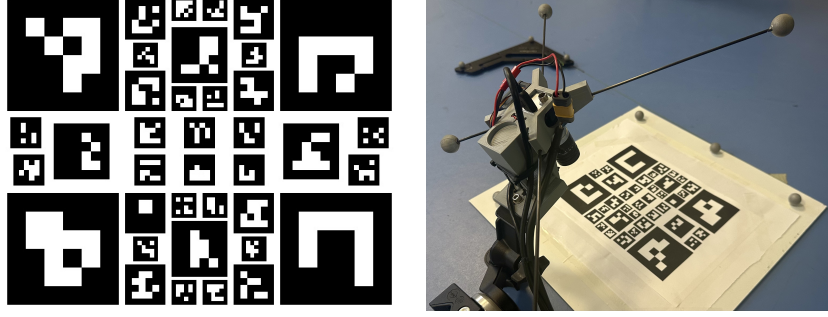


Figure 2: (left) The arrangement of fiducial markers on the planar target. (right) The camera and target with attached MoCap markers.

target (the setup is shown in Fig. 2). The key advantage of using the ArUco markers is that a single marker provides enough correspondences, via the coordinates of its four corner, to compute the camera's relative pose.

This setup replicates the scenario of a drone equipped with a camera observing a planar landing marker, where it initially starts from a distant position and then performs a range of motion and orientation changes as it gradually moves closer to the target. While the target was downscaled by a factor of four for the experiment due to the MoCap system's limited tracking volume, in a real deployment, the estimated position would scale with the target's actual size.

#### 4.1 Results and discussion

Figures 3 and 4 show the estimated camera relative position and attitude (represented by the corresponding Euler angles) obtained using the proposed algorithm with algebraic averaging of  $\hat{\eta}$  (relation (7)) and the smooth averaging (relation (9)), compared to the ground truth obtained from the MoCap system. While the overall motion is consistent with the ground truth, the pitch and roll estimates (related to unit normal vector) provided by the proposed solution with algebraic averaging exhibit significant noise, particularly when the camera is far from the target (i.e., for larger  $\xi_3$ ), as the detected marker corners appear closer in the image. Using smooth averaging significantly reduces this noise and improves the attitude estimation.

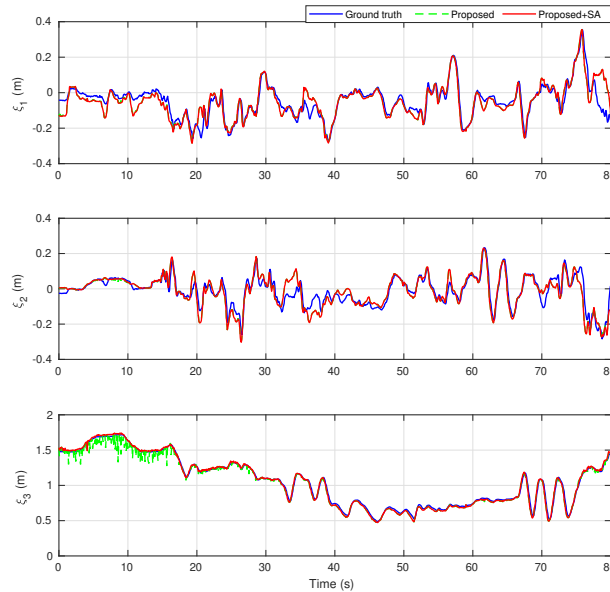


Figure 3: Camera relative positions w.r.t the target given by the proposed algorithm without smoothing (green), with the smooth averaging (red), and MoCap ground truth (blue).

The estimated pose obtained with the proposed method with smooth averaging was benchmarked against two solvers implemented in OpenCV's *solvePnP()* function: an iterative *PnP* solver using the classical Levenberg-Marquardt (LM) optimization method initialized via homography decomposition, and the *EPnP* algorithm.

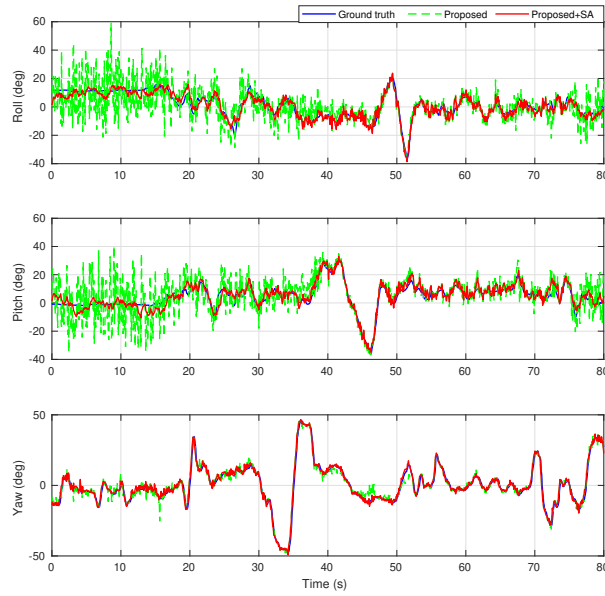


Figure 4: Camera relative attitude (Euler angles) w.r.t the target given by the proposed algorithm without smoothing (green), with the smooth averaging (red), and MoCap ground truth (blue).

Figures 5 and 6 show the estimated camera position and attitude (Euler angles) obtained using the proposed method with smooth averaging,  $EPnP$ , and Iterative (LM), compared to the MoCap ground truth. The results demonstrate that the three methods achieve similar results overall. However, the  $EPnP$  algorithm occasionally fails to produce valid estimates, and both  $EPnP$  and LM yield noticeably noisier pitch and roll estimates at larger distances (e.g., 0-20s), the proposed method with smooth averaging provides consistent estimates across the entire sequence.

Table 1 reports the root mean square error (RMSE) for the position and orientation estimates obtained with each method. Orientation errors are computed from Euler angle deviations relative to the MoCap ground truth. Although all methods achieve similar orientation accuracy, with the LM method achieving the lowest angular error, the proposed method yields the lowest position RMSE and significantly outperforms both  $EPnP$  and LM.

Table 1: Pose estimation RMSE compared to MoCap ground truth.

Method	Position RMSE (m)	Orientation RMSE (deg)
Iterative (LM)	0.1574	<b>5.2766</b>
$EPnP$ Lepetit et al. [2009]	0.1773	5.4194
Proposed	<b>0.0623</b>	5.3527

## 5 Conclusions

In this paper, we addressed the problem of estimating the pose of a camera relative to a planar target from planar point features and their corresponding bearing measurements. The proposed algebraic approach estimates the pose hierarchically and guarantees good estimates of the position direction vector even when the camera orientation is poorly estimated. To improve the method's robustness to pixel noise, a smooth averaging formulation was introduced to refine the estimation of the target's normal. Extensive experiments demonstrate the accuracy and reliability of the method. The primary motivation for this work is its potential application to vision-based control of autonomous drone landing on planar targets. Future work will focus on extending the approach to moving targets by combining data from an onboard IMU.

## Acknowledgment

This work has been supported by the "Grands Fonds Marins" Project Deep-C, and the ASTRID ANR project ASCAR.



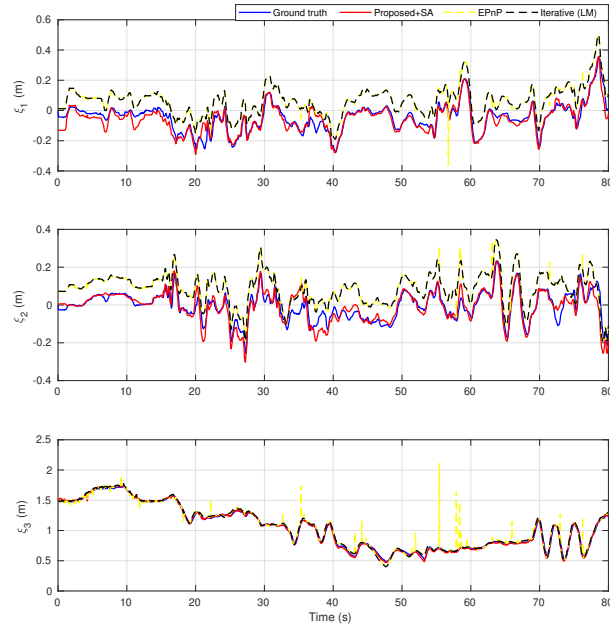


Figure 5: Camera relative positions w.r.t the target given by the proposed algorithm (red), the EPnP (yellow), iterative PnP (black) and MoCap ground truth (blue).

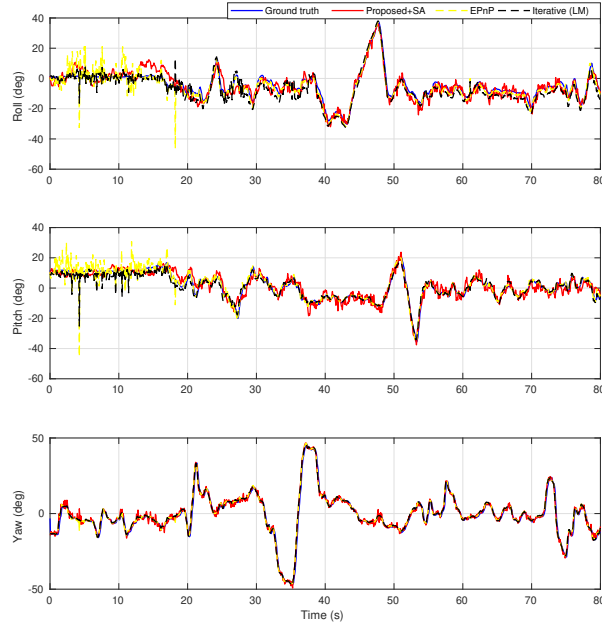


Figure 6: Camera relative attitudes (Euler angles) w.r.t the target given by the proposed algorithm (red), the EPnP (yellow), iterative PnP (black) and MoCap ground truth (blue).

## References

- Martin A Fischler and Robert C Bolles. Random sample consensus: a paradigm for model fitting with applications to image analysis and automated cartography. *Communications of the ACM*, 24(6):381–395, 1981.
- Xiao-Shan Gao, Xiao-Rong Hou, Jianliang Tang, and Hang-Fei Cheng. Complete solution classification for the perspective-three-point problem. *IEEE transactions on pattern analysis and machine intelligence*, 25(8):930–943, 2003.

- Laurent Kneip, Davide Scaramuzza, and Roland Siegwart. A novel parametrization of the perspective-three-point problem for a direct computation of absolute camera position and orientation. In *CVPR 2011*, pages 2969–2976. IEEE, 2011.
- Cai-Xia Zhang and Zhan-Yi Hu. A general sufficient condition of four positive solutions of the p3p problem. *Journal of Computer Science and Technology*, 20(6):836–842, 2005.
- Long Quan and Zhongdan Lan. Linear n-point camera pose determination. *IEEE Transactions on pattern analysis and machine intelligence*, 21(8):774–780, 1999.
- Robert M Haralick, Hyonam Joo, Chung-Nan Lee, Xinhua Zhuang, Vinay G Vaidya, and Man Bae Kim. Pose estimation from corresponding point data. *IEEE Transactions on Systems, Man, and Cybernetics*, 19(6):1426–1446, 1989.
- Daniel F DeMenthon and Larry S Davis. Model-based object pose in 25 lines of code. *International journal of computer vision*, 15:123–141, 1995.
- C-P Lu, Gregory D Hager, and Eric Mjolsness. Fast and globally convergent pose estimation from video images. *IEEE transactions on pattern analysis and machine intelligence*, 22(6):610–622, 2000.
- Gerald Schweighofer and Axel Pinz. Globally optimal  $O(n)$  solution to the pnp problem for general camera models. In *BMVC*, pages 1–10. Citeseer, 2008.
- Vincent Lepetit, Francesc Moreno-Noguer, and Pascal Fua. Ep n p: An accurate  $O(n)$  solution to the p n p problem. *International journal of computer vision*, 81:155–166, 2009.
- Joel A Hesch and Stergios I Roumeliotis. A direct least-squares (dls) method for pnp. In *2011 International Conference on Computer Vision*, pages 383–390. IEEE, 2011.
- Shiqi Li, Chi Xu, and Ming Xie. A robust  $O(n)$  solution to the perspective-n-point problem. *IEEE transactions on pattern analysis and machine intelligence*, 34(7):1444–1450, 2012.
- Laurent Kneip, Hongdong Li, and Yongduek Seo. Upnp: An optimal  $O(n)$  solution to the absolute pose problem with universal applicability. In *Computer Vision—ECCV 2014: 13th European Conference, Zurich, Switzerland, September 6–12, 2014, Proceedings, Part I 13*, pages 127–142. Springer, 2014.
- Tarek Hamel and Claude Samson. Riccati observers for the nonstationary pnp problem. *IEEE Transactions on Automatic Control*, 63(3):726–741, 2017.
- Denis Oberkampf, Daniel F DeMenthon, and Larry S Davis. Iterative pose estimation using coplanar feature points. *Computer Vision and Image Understanding*, 63(3):495–511, 1996.
- Gerald Schweighofer and Axel Pinz. Robust pose estimation from a planar target. *IEEE transactions on pattern analysis and machine intelligence*, 28(12):2024–2030, 2006.
- Toby Collins and Adrien Bartoli. Infinitesimal plane-based pose estimation. *International journal of computer vision*, 109(3): 252–286, 2014.
- Richard Hartley and Andrew Zisserman. *Multiple view geometry in computer vision*. Cambridge university press, 2003.
- Olivier D Faugeras and Francis Lustman. Motion and structure from motion in a piecewise planar environment. *International Journal of Pattern Recognition and Artificial Intelligence*, 2(03):485–508, 1988.
- Zhongfei Zhang and Allen R Hanson. 3d reconstruction based on homography mapping. *Proc. ARPA96*, pages 1007–1012, 1996.
- Ezio Malis and Manuel Vargas. *Deeper understanding of the homography decomposition for vision-based control*. PhD thesis, Inria, 2007.
- Francisco J Romero-Ramirez, Rafael Muñoz-Salinas, and Rafael Medina-Carnicer. Speeded up detection of squared fiducial markers. *Image and vision Computing*, 76:38–47, 2018.